

Proposed Coupling of an Electron Spin in a Semiconductor Quantum Dot to a Nanosize Optical Cavity

Arka Majumdar,^{1,*} Per Kaer,² Michal Bajcsy,¹ Erik D. Kim,¹ Konstantinos G. Lagoudakis,¹
Armand Rundquist,¹ and Jelena Vučković¹

¹*E.L.Ginzton Laboratory, Stanford University, Stanford, California 94305, USA*

²*DTU Fotonik, Department of Photonics Engineering, Technical University of Denmark, Building 345W, 2800 Kgs. Lyngby, Denmark*

(Received 23 November 2012; published 9 July 2013)

We propose a scheme to efficiently couple a single quantum dot electron spin to an optical nano-cavity, which enables us to simultaneously benefit from a cavity as an efficient photonic interface, as well as to perform high fidelity (nearly 100%) spin initialization and manipulation achievable in bulk semiconductors. Moreover, the presence of the cavity speeds up the spin initialization process beyond the GHz range.

DOI: [10.1103/PhysRevLett.111.027402](https://doi.org/10.1103/PhysRevLett.111.027402)

PACS numbers: 78.67.Hc, 03.67.Hk, 42.50.Pq, 85.35.Be

Single quantum emitters coupled to optical cavities constitute a platform that allows conversion of quantum states of one physical system to those of another in an efficient and reversible manner. Such cavity quantum electrodynamic systems have been the subject of intense studies as one of the building blocks for scalable quantum information processing and long distance quantum communication [1,2]. Over the years, these systems have evolved from conventional atomic systems [3] to include those based on solid state emitters, including quantum dots [4,5]. Although, significant progress has been made in quantum-dot-(QD-)based cavity quantum electrodynamics [6–12], most of the reported works use a neutral QD, which effectively acts as a two-level quantum emitter with an optical transition from the ground state to the single exciton state. While such a two-level system could in principle be used as a qubit [13,14], the short lifetime of the exciton state (<1 ns) makes it not suitable for practical applications.

On the other hand, the spin states of a singly charged QD have been shown to possess coherence times in the microsecond range [15,16]. The use of ultrafast optical techniques with charged QDs provides the possibility of performing a very high number of spin manipulations within the spin coherence time and opens avenues for their use as qubits for quantum information applications [15,16]. However, the efficiency of spin initialization [17] and manipulation achieved so far is not high. To attain the efficiency necessary for practical applications, one needs to enhance the light-matter interaction. This can be achieved by embedding the charged QD in a cavity. Several groups have so far demonstrated deterministic charging of a single QD within a photonic crystal cavity [18,19] and magnetic field tuning of a single QD strongly coupled to a photonic crystal cavity [14]. Recently, manipulation of a QD spin in a linearly polarized photonic crystal cavity was reported by Carter *et al.* [20]. However, the configuration used in their approach does not permit getting full advantage of the photonic interface as the

cavity supports only one polarization, whereas the QD-spin transitions are of two different polarizations. Moreover, the spin initialization is performed for a far detuned QD-cavity system, where the enhancement due to a cavity is not maximized.

In this Letter, we theoretically analyze a system consisting of a QD spin coupled to a nanocavity, with realistic system parameters. While one might naively think that coupling a QD spin to a cavity is a simple extension of coupling a neutral QD to a cavity, a closer look quickly reveals that it is not so. Specifically, the QD spin states become significantly perturbed due to the presence of the cavity, and the spin initialization or control becomes impossible when the cavity is brought on resonance with QD transitions in an attempt to enhance them. In this work, we show how this can be overcome and that successful QD spin initialization and manipulation can be achieved in a properly chosen configuration based on a bimodal nanocavity [see Fig. 1(a)]. Bimodal photonic crystal nanocavities were previously proposed for nonclassical light generation and near-degenerate bimodal cavities were also demonstrated [21,22]. We analyze a large parameter space and find an optimal range of detunings between QD transitions, cavity modes, and the driving laser for which a high fidelity of spin initialization can be achieved. The presence of a cavity also increases the speed of spin initialization by enhancing the rates of the coupled transitions, bringing it to beyond the GHz range that is not achievable in bulk semiconductors [15]. Finally we describe the spin manipulation in such a system. Here, we find that coherent population transfer is realized only by applying a short optical pulse that is far detuned from the QD-cavity system.

Previously, several research articles looked theoretically into the problem of spin initialization and manipulation in a cavity [23–26]. However, in those studies, it was assumed that the effect of the cavity is mainly to enhance the local electric field of a laser and that the QD is driven by a classical field. This assumption breaks down for a QD

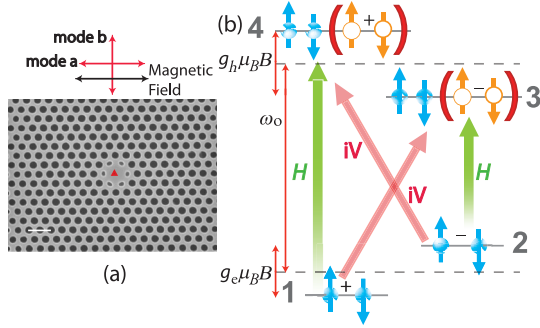


FIG. 1 (color online). (a) Scanning electron microscope image of a bimodal photonic-crystal nanocavity fabricated in a GaAs membrane with embedded quantum dots. The scale bar is 500 nm. Due to the C_6 symmetry of the cavity, it can support two orthogonally polarized near-degenerate modes. (b) The schematics and the optical transitions of a four-level system arising when a magnetic field is applied in the Voigt configuration [plot (a)] to a QD charged with a single electron. The states $|1\rangle$ and $|2\rangle$ are superpositions of electron spin up and down, and the states $|3\rangle$ and $|4\rangle$ are trion states with both electron spins and superposition of hole spins. The cavity mode a has H polarization [plot (a)] and can couple to transitions $|1\rangle \rightarrow |4\rangle$ and $|2\rangle \rightarrow |3\rangle$, while the cavity mode b has V polarization and can drive the transitions $|1\rangle \rightarrow |3\rangle$ and $|2\rangle \rightarrow |4\rangle$.

embedded in a high- Q photonic cavity and therefore quantization of the cavity field and a careful choice of driving terms are important for a realistic treatment of the coupled system. A single electron spin confined to the QD can be in two different states of the same energy: spin up or spin down, where we define the spin state along the optical axis (QD growth, i.e., z axis). When a magnetic field is applied perpendicularly to the optical axis (also known as the Voigt geometry), the spin-up and spin-down states split by an amount $\Delta_e = g_e \mu_B B$ [see Fig. 1(b)]. These states can also be thought of as spin-up and spin-down states along the x axis, and we will use this notation for the rest of the Letter. The excited state of the QD, called the trion state, also splits. The excited state splitting is due to the hole spin and is given by $\Delta_h = g_h \mu_B B$. Here g_e and g_h are, respectively, the Lande g factor for electrons and holes, μ_B is the Bohr magneton, B is the applied magnetic field, and in this work we neglect any diamagnetic shift of the QD. The lossless dynamics of the system consisting of QD spins coupled to a cavity with two modes of perpendicular polarizations [labeled H and V in Fig. 1(b)] and driven by a laser can be described by the Hamiltonian $\mathcal{H} = \mathcal{H}_0 + \mathcal{H}_{\text{int}} + \mathcal{H}_d$, where under the rotating-wave approximation (and with $\hbar = 1$)

$$\begin{aligned} \mathcal{H}_0 = & -\frac{\Delta_e}{2}|1\rangle\langle 1| + \frac{\Delta_e}{2}|2\rangle\langle 2| + \left(\omega_0 - \frac{\Delta_h}{2}\right)|3\rangle\langle 3| \\ & + \left(\omega_0 + \frac{\Delta_h}{2}\right)|4\rangle\langle 4| + \omega_a a^\dagger a + \omega_b b^\dagger b, \end{aligned} \quad (1)$$

$$\mathcal{H}_{\text{int}} = g_a a^\dagger (\sigma_{14} + \sigma_{23}) + i g_b b^\dagger (\sigma_{24} + \sigma_{13}) + \text{H.c.} \quad (2)$$

Here, g_a and g_b describe the coupling strengths between the cavity modes and the QD transitions, a and b are the photon annihilation operators of the two cavity modes with frequencies ω_a and ω_b , respectively, $\sigma_{ij} = |i\rangle\langle j|$, and ω_0 is the frequency of the QD's optical transitions in the absence of the magnetic field [see Fig. 1(b)]. The driving part of the Hamiltonian \mathcal{H}_d changes depending on whether the applied laser field drives the QD or the cavity. We consider the general form of the driving Hamiltonian ($\mathcal{H}_d = \mathcal{H}_d^{\text{cav}} + \mathcal{H}_d^{\text{QD}}$), which describes a single laser with controllable polarization capable of driving both the cavity modes ($\mathcal{H}_d^{\text{cav}}$) or the QD directly ($\mathcal{H}_d^{\text{QD}}$):

$$\mathcal{H}_d^{\text{cav}} = \mathcal{E}_a e^{i\omega_l t} a + \mathcal{E}_b e^{i\omega_l t} b + \text{H.c.}, \quad (3)$$

where $\mathcal{E}_{a,b}$ are the rates with which the applied laser field excites each of the cavity modes, and

$$\mathcal{H}_d^{\text{QD}} = \Omega_h e^{i\omega_l t} (\sigma_{13} + \sigma_{24}) + \Omega_v e^{i\omega_l t} (\sigma_{23} + \sigma_{14}) + \text{H.c.} \quad (4)$$

Here, Ω_h and Ω_v are the Rabi frequencies of the laser for the horizontal and the vertical QD transitions, respectively. Depending on the driving conditions, one of the two terms in \mathcal{H}_d can be dominant. For example, if a laser can couple to cavity resonance, we assume that $\mathcal{H}_d^{\text{cav}}$ is dominant, and neglect $\mathcal{H}_d^{\text{QD}}$. In other words, the QD is always driven via a cavity mode. This condition is assumed for spin initialization. On the other hand, if the laser cannot couple well to cavity resonance, but QD transitions are instead driven directly, $\mathcal{H}_d^{\text{QD}}$ dominates. This happens when the laser detuning from QD transitions is smaller than from cavity resonances [27], or when the laser is applied from the spatial direction where it does not couple to cavity modes. In this Letter, we show that for coherent spin manipulation, it is necessary to drive the QD directly, and not via a cavity mode. We can transform the Hamiltonian into the rotating frame by using $\mathcal{H}_r = T^\dagger \mathcal{H} T + i(\partial T^\dagger / \partial t) T$ where $T = e^{-i\omega_l t (a^\dagger a + b^\dagger b + |3\rangle\langle 3| + |4\rangle\langle 4|)}$.

The losses in the system are incorporated by solving the master equation of the density matrix ρ of the coupled QD-cavity system: $d\rho/dt = -i[\mathcal{H}_r, \rho] + \sum_j \mathcal{L}(c_j)$, where $\mathcal{L}(c_j) = 2c_j \rho c_j^\dagger - c_j^\dagger c_j \rho - \rho c_j^\dagger c_j$ is the Lindblad operator for the collapse operator c_j . In this case, we have six different loss channels, and hence six collapse operators (one for each cavity and each QD transition): $c_j \in \{\sqrt{\kappa}a, \sqrt{\kappa}b, \sqrt{\gamma_{41}}\sigma_{41}, \sqrt{\gamma_{42}}\sigma_{42}, \sqrt{\gamma_{31}}\sigma_{31}, \sqrt{\gamma_{32}}\sigma_{32}\}$.

We now use this model to theoretically investigate the spectrum of the coupled charged QD-cavity system probed under photoluminescence (PL) as is commonly done experimentally (to reveal eigenstates of the system). We perform this analysis for two different cavity decay rates: the readily achievable cavity decay rate $\kappa/2\pi = 20$ GHz

and better than the state of the art (but achievable with cavity fabrication improvements) system parameters with $\kappa/2\pi = 5$ GHz. The dot-cavity interaction strength is $g/2\pi = 20$ GHz for both cases (corresponding to experimentally achievable conditions [28]). The dipole decay rates are $\gamma_{41}, \gamma_{42}, \gamma_{31}, \gamma_{32}/2\pi = 1$ GHz. When the system is characterized through PL, an above band laser pumps the semiconductor to generate electron hole pairs. These carriers recombine in the QD, which subsequently emits a photon. This is an incoherent way of probing the system, and is modeled by adding Lindblad terms $P(\mathcal{L}(a^\dagger) + \mathcal{L}(b^\dagger))$, which signify incoherently populating the cavities with a rate P . A low value of $P/2\pi \sim 0.1$ is used to allow using a small Fock state basis ($N = 4$). We calculate the power spectral density (PSD) $S(\omega)$ of the system given by $S(\omega) = \int_{-\infty}^{\infty} \langle a^\dagger(t)a \rangle e^{-i\omega t} + \langle b^\dagger(t)b \rangle e^{-i\omega t} dt$, where ω is the spectrometer frequency, and in the rotating frame $\Delta = \omega - \omega_0$. The numerically simulated PSD as a function of increasing magnetic field is shown in Fig. 2 for two different values of the cavity decay rates $\kappa/2\pi = 5$ and 20 GHz. Peaks in the PSD correspond to eigenstates of the coupled system. For a system with low κ , we observe six peaks (for $B > 0$). However, with increasing cavity decay rates, the energies of the eigenstates become degenerate and such structure disappears. To understand the origin of the six peaks, we note that with one quantum of energy present in the system, the bare states of the coupled charged QD-bimodal cavity system are $|1, 0, 1\rangle, |0, 1, 1\rangle, |1, 0, 2\rangle, |0, 1, 2\rangle, |0, 0, 3\rangle$, and $|0, 0, 4\rangle$, where the first number denotes the number of photons present in the mode a , the second number is the number of photons in mode b , and the last one is the populated charged QD state. If g/κ is sufficiently large, these bare states couple and give rise to six dressed states that we observe in the PL spectrum in Fig. 2(a). For additional intuitive understanding, we diagonalize the

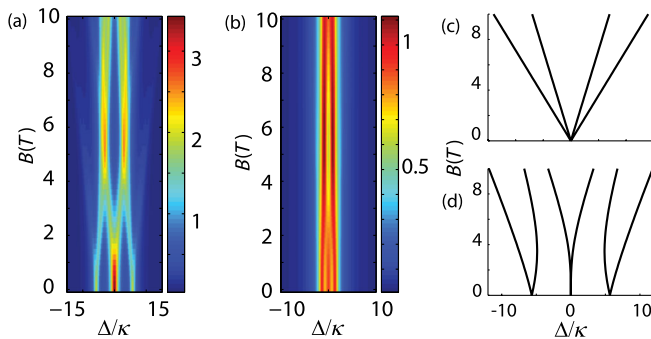


FIG. 2 (color online). Photoluminescence spectra of the coupled QD spin-cavity system as a function of the magnetic field (a) for a QD-cavity system with $\kappa/2\pi = 5$ GHz and $g/2\pi = 20$ GHz. (b) Similar PL spectra for $g/2\pi = \kappa/2\pi = 20$ GHz. (c), (d) Energy splitting between all the QD transitions as a function of the magnetic field without (c) and with (d) a cavity in the absence of losses ($\kappa = 0$).

Hamiltonian when only one photon is present in the system and plot the eigenvalues as a function of the magnetic field. In the absence of the cavity, we see four transitions from the QD [see Fig. 2(c)]. In the presence of the two cavity modes, however, a hybridization between the cavity modes and the QD transitions occurs, which results in six observable transitions [see Fig. 2(d)]. We note that these six transitions are also present in the system with larger cavity losses [see Fig. 2(b)], but they cannot be as clearly resolved as in Fig. 2(a) because of their overlap.

Next, we proceed to study the spin initialization in such a QD-cavity system. We analyze the speed and fidelity of spin initialization as a function of laser and cavity detuning. We consider the state of the art parameter set for these simulations ($\kappa/2\pi = 20$ GHz and $g/2\pi = 20$ GHz) and assume a magnetic field of 5 T, resulting in $\Delta_e/2\pi \approx 28$ GHz and $\Delta_h/2\pi \approx 14$ GHz. We also assume that the QD spin starts in a mixed state with equal spin-up and spin-down (i.e., equal states $|1\rangle$ and $|2\rangle$) population: $\rho_{11} = \rho_{22} = 1/2$. We pump the system with an H -polarized laser (which couples to mode a), while the other (V -polarized) cavity mode b is not driven. In other words, we use the laser to drive outer (H) transitions in Fig. 1(b) via cavity mode a , but the inner (V) polarized QD transitions are coupled to the vacuum field of the cavity mode b . For each Λ QD system, this resembles the vacuum induced transparency (VIT) configuration recently proposed and experimentally studied in atomic physics [29]. Figure 3(a) plots $|\rho_{11} - \rho_{22}|$ as a function of the pump laser wavelength and the cavity mode b frequency ω_b . The cavity mode a

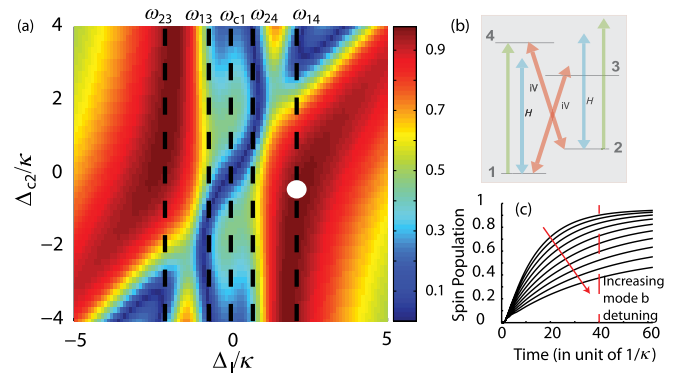


FIG. 3 (color online). (a) Initialization fidelity $|\rho_{11} - \rho_{22}|$ as a function of the cavity mode b frequency $\Delta_b = \omega_b - \omega_0$ and the pump laser wavelength $\Delta_l = \omega_l - \omega_0$. The white point marks the situation where we get optimal spin initialization fidelity [the situation shown in (b)]: the pump laser is tuned to the QD transition $|1\rangle \rightarrow |4\rangle$, and the cavity mode b is tuned to the transition $|2\rangle \rightarrow |4\rangle$. Here the double arrows denote cavity fields and the single arrows denote the laser. (c) The spin initialization as a function of time for different cavity detunings Δ_{c2} , with the laser being fixed at the transition frequency $\omega_{14}(\Delta_l \sim 2\kappa)$. Δ_{c2} is changed from 0 to 2κ . We note that the spin-initialization time is only around $40/\kappa \sim 300$ ps. Parameters for simulation: $g/2\pi = \kappa/2\pi = 20$ GHz at a magnetic field of 5 T.

frequency ω_a is kept fixed at ω_0 (QD transition in the absence of the B field, see Fig. 1), so the laser is not necessarily on resonance with this mode. We find that a high fidelity spin initialization is achieved when the pump laser is tuned to the QD transition $|1\rangle \rightarrow |4\rangle$, and the cavity mode b (which is in the vacuum state) is tuned to the transition $|2\rangle \rightarrow |4\rangle$ [see Fig. 3(b)]. The laser can potentially couple to the transition $|2\rangle \rightarrow |3\rangle$ and the cavity mode b to the transition $|1\rangle \rightarrow |3\rangle$. However, due to detunings of the laser and the cavity mode b , the QD is efficiently optically pumped only via the $|1\rangle \rightarrow |4\rangle \rightarrow |2\rangle$ route, leading to all the spin population being in the QD state $|2\rangle$. In a similar fashion we can also use the path $|2\rangle \rightarrow |3\rangle \rightarrow |1\rangle$, with a different set of detunings to achieve initialization in state $|1\rangle$. Figure 3(a) also reveals that a high spin initialization fidelity can also be achieved when the cavity is far detuned [20], but this is a trivial case equivalent to the situation of a QD uncoupled to the cavity (a QD in bulk semiconductors), eliminating the cavity's beneficial role.

Next, we focus on the temporal dynamics of the spin population with varying detuning ω_b of the cavity mode b . We observe that the spin initialization is faster when the cavity is resonant to the $|2\rangle \rightarrow |4\rangle$ transition [see Fig. 3(c)]. The initialization speed of several GHz is achieved in this case, but even faster initialization speed can be achieved by pumping the system with a stronger laser (while keeping a resonant cavity on the other transition in the Λ system). We note that such speed is almost one order of magnitude larger than the previously reported result for a bare QD [17]. The simulations were performed using the open source Python package QuTip [30].

Finally we analyze how the spin manipulation can be performed in such a system. The coupled QD-cavity system is driven by a laser pulse with different detunings, and the spin population is monitored as a function of the pulse amplitude. Initially all the population is in state $|1\rangle$. We assume that the cavity is at the undressed QD frequency ω_0 , and we drive the QD directly (i.e., the driving conditions are such that the laser is spatially or spectrally decoupled from cavity modes) (see the Supplemental Material [31]). The system is excited with a short pulse (pulse width 5 ps), and the spin population in states $|1\rangle$ (ρ_{11}) and $|2\rangle$ (ρ_{22}) is monitored over time (see the Supplemental Material [31]). The spin population difference ($\rho_{11} - \rho_{22}$) in the steady state is plotted as a function of the pulse amplitude for three different pulse detunings Δ from the cavity resonances [see Fig. 4(a)]. Rabi oscillations are observed between the spin-up ($|1\rangle$) and spin-down ($|2\rangle$) states as the pulse amplitude is changed. To check whether the process is coherent, we calculate the trace of the density matrix $\rho^{(1,2)}$ of the subspace consisting of spin-up and spin-down states, and plot $\text{Tr}[(\rho^{(1,2)})^2]$ in Fig. 4(b). $\text{Tr}[(\rho^{(1,2)})^2]$ is unity for a pure state. Therefore, if the spin manipulation process is coherent, we expect this value to be near unity. Our results in Fig. 4(b) indicate that only at a

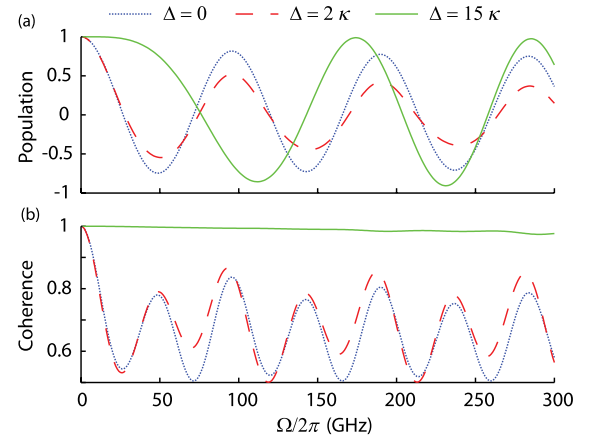


FIG. 4 (color online). (a) The steady-state spin population ($\rho_{11} - \rho_{22}$) as a function of the laser Rabi frequency ($\Omega_h = \Omega_v$). All the population is initially in state $|1\rangle$, and a 5 ps laser pulse excites the system. Three different pulse detunings are used. Rabi oscillations between two spin states are observed. (b) $\text{Tr}[(\rho^{(1,2)})^2]$ as a function of the laser Rabi frequency. The process becomes coherent [$\text{Tr}[(\rho^{(1,2)})^2] \sim 1$] when the detuning of the pulse from the QD-cavity system is large. Parameters for simulation: $g/2\pi = \kappa/2\pi = 20$ GHz at a magnetic field of 5 T.

large detuning Δ is the process coherent. Additionally, the process is only coherent if the QD is driven directly (and not via a cavity) (see the Supplemental Material [31]). Therefore, a coherent spin manipulation in the proposed system is also possible, but only by applying an optical pulse that is far detuned from the cavity and drives the QD directly.

In summary, we have presented a proposal for efficient initialization and manipulation of a single QD spin coupled to a bimodal optical cavity. Our numerical analysis (with full field quantization and with realistic system parameters) confirms that nearly 100% spin initialization fidelity is achievable with a speed beyond the GHz range, as well as spin manipulation, benefiting from a cavity not only as a photonic interface but also to speed up the spin control.

The authors acknowledge financial support provided by the Air Force Office of Scientific Research, MURI Center for Multifunctional Light-Matter Interfaces Based on Atoms and Solids. K. G. L. acknowledges support by the Swiss National Science Foundation and A. R. is also supported by a Stanford Graduate Fellowship.

*Present address: Physics Department, University of California, Berkeley, California 94720, USA.
arka.majumdar@berkeley.edu

- [1] H. J. Kimble, *Nature (London)* **453**, 1023 (2008).
- [2] S. Ritter, C. Nölleke, C. Hahn, A. Reiserer, A. Neuzner, M. Uphoff, M. Mücke, E. Figueroa, J. Bochmann, and G. Rempe, *Nature (London)* **484**, 195 (2012).
- [3] H. J. Kimble, in *Cavity Quantum Electrodynamics*, edited by P. Berman (Academic, New York, 1994).

- [4] T. Yoshie, A. Scherer, J. Hendrickson, G. Khitrova, H. M. Gibbs, G. Rupper, C. Ell, O.B. Shchekin, and D.G. Deppe, *Nature (London)* **432**, 200 (2004).
- [5] A. Faraon, A. Majumdar, D. Englund, E. Kim, M. Bajcsy, and J. Vučković, *New J. Phys.* **13**, 055025 (2011).
- [6] A. Faraon, I. Fushman, D. Englund, N. Stoltz, P. Petroff, and J. Vučković, *Nat. Phys.* **4**, 859 (2008).
- [7] A. Majumdar, M. Bajcsy, and J. Vučković, *Phys. Rev. A* **85**, 041801 (2012).
- [8] A. Reinhard, T. Volz, M. Winger, A. Badolato, K.J. Hennessy, E.L. Hu, and A. Imamoglu, *Nat. Photonics* **6**, 93 (2012).
- [9] A. Faraon, A. Majumdar, H. Kim, P. Petroff, and J. Vučković, *Phys. Rev. Lett.* **104**, 047402 (2010).
- [10] D. Englund, A. Majumdar, M. Bajcsy, A. Faraon, P. Petroff, and J. Vučković, *Phys. Rev. Lett.* **108**, 093604 (2012).
- [11] D. Sridharan *et al.*, [arXiv:1107.3751v1](https://arxiv.org/abs/1107.3751v1).
- [12] T. Volz, A. Reinhard, M. Winger, A. Badolato, K.J. Hennessy, E.L. Hu, and A. Imamoglu, *Nat. Photonics* **6**, 605 (2012).
- [13] V. Jovanov *et al.*, *Proc. SPIE Int. Soc. Opt. Eng.* **8272**, 827211(2012).
- [14] H. Kim, R. Bose, T.C. Shen, G.S. Solomon, and E. Waks, *Nat. Photonics* **7**, 373 (2013).
- [15] D. Press, T.D. Ladd, B. Zhang, and Y. Yamamoto, *Nature (London)* **456**, 218 (2008).
- [16] E.D. Kim, K. Truex, X. Xu, B. Sun, D.G. Steel, A.S. Bracker, D. Gammon, and L.J. Sham, *Phys. Rev. Lett.* **104**, 167401 (2010).
- [17] X. Xu, Y. Wu, B. Sun, Q. Huang, J. Cheng, D.G. Steel, A.S. Bracker, D. Gammon, C. Emary, and L.J. Sham, *Phys. Rev. Lett.* **99**, 097401 (2007).
- [18] D. Pinotsi, P. Fallahi, J. Miguel-Sanchez, and A. Imamoglu, *IEEE J. Quantum Electron.* **47**, 1371 (2011).
- [19] A. Laucht, F. Hofbauer, N. Hauke, J. Angele, S. Stobbe, M. Kaniber, G. Böhm, P. Lodahl, M.-C. Amann, and J. J. Finley, *New J. Phys.* **11**, 023034(2009).
- [20] S.G. Carter, T.M. Sweeney, M. Kim, C.S. Kim, D. Solenov, S.E. Economou, T.L. Reinecke, L. Yang, A.S. Bracker, and D. Gammon, *Nat. Photonics* **7**, 329 (2013).
- [21] K. Hennessy, C. Hogerle, E. Hu, A. Badolato, and A. Imamoglu, *Appl. Phys. Lett.* **89**, 041118 (2006).
- [22] A. Majumdar, M. Bajcsy, A. Rundquist, and J. Vučković, *Phys. Rev. Lett.* **108**, 183601 (2012).
- [23] V. Loo, L. Lanco, O. Krebs, P. Senellart, and P. Voisin, *Phys. Rev. B* **83**, 033301 (2011).
- [24] A. Majumdar, Z. Lin, A. Faraon, and J. Vučković, *Phys. Rev. A* **82**, 022301 (2010).
- [25] A. Imamoglu, D.D. Awschalom, G. Burkard, D.P. DiVincenzo, D. Loss, M. Sherwin, and A. Small, *Phys. Rev. Lett.* **83**, 4204 (1999).
- [26] M. Feng, I. D'Amico, P. Zanardi, and F. Rossi, *Phys. Rev. A* **67**, 014306 (2003).
- [27] A. Majumdar, A. Papageorge, E.D. Kim, M. Bajcsy, H. Kim, P. Petroff, and J. Vučković, *Phys. Rev. B* **84**, 085310 (2011).
- [28] D. Englund, A. Majumdar, A. Faraon, M. Toishi, N. Stoltz, P. Petroff, and J. Vučković, *Phys. Rev. Lett.* **104**, 073904 (2010).
- [29] H. Tanji-Suzuki, W. Chen, R. Landig, J. Simon, and V. Vuletic, *Science* **333**, 1266 (2011).
- [30] J. Johansson, P.D. Nation, and F. Nori, *Comput. Phys. Commun.* **184**, 1234 (2013).
- [31] See the Supplemental Material at <http://link.aps.org/supplemental/10.1103/PhysRevLett.111.027402> for a discussion on the modeling of QD and cavity driving.